tions are much less affected by differences in temperature than the average values. This implies that, at room temperature, a relatively large fraction of the observed bond lengths is only marginally influenced by thermal motions.

For the methyl group, bond shortening reduces only slowly upon cooling and is still significant at liquid-nitrogen temperatures. We associate this with the rotational freedom of the methyl group. For the other connectivities at $T \sim 100$ K, the observed bond lengths have already (or almost) reached the spectroscopically determined values (Fig. 3).

'True' chemical differences of C–H bond lengths in different connectivities are best studied at liquid-helium temperatures, but can also be observed at room temperature (Fig. 2). In general, the C–H bond length should increase with increasing (positive) partial charge on the C atom. This is actually observed in the present data set (Table 2), where the longest $\langle d_{CH} \rangle$ is found for connectivity (5).

This study was supported by the Bundesministerium für Forschung und Technologie, FKZ 03 SA3 FUB, and by the Fonds der Chemischen Industrie.

References

ALLEN, F. H. (1986). *Acta Cryst.* B**42**, 515–522.
ALLEN, F. H., BELLARD, S., BRICE, M. D., CARTWRIGHT, B. A., DOUBLEDAY, A., HIGGS, H., HUMMELINK, T., HUMMELINK-PETERS, B. G., KENNARD, O., MOTHERWELL, W. D. S., RODGERS, J. R. & WATSON, D. G. (1979). *Acta Cryst.* B**35**, 2331–2339.
BUSING, W. R. & LEVY, H. A. (1964). *Acta Cryst.* **17**, 142–146.
CALLOMAN, J. H., HIROTA, E., KUCHITSU, K., LAFFERTY, W. J., MAKI, A. G. & POTE, C. S. (1976). *Structure Data of Free Polyatomic Molecules. Landolt-Börnstein, Numerical Data and Functional Relationships in Science and Technology*, New Series, Group II, Vol. 7. Berlin: Springer Verlag.
CRAVEN, B. M. & SWAMINATHAN, S. (1984). *Trans. Am. Crystallogr. Assoc.* **23**, 71–81.
DUNITZ, J. D. & WHITE, D. N. J. (1973). *Acta Cryst.* A**29**, 93–94.
JEFFREY, G. A., RUBLE, J. R., MCMULLAN, R. K., DEFREES, D. J. & POPLE, J. A. (1981). *Acta Cryst.* B**37**, 1885–1890.
JOHNSON, C. K. & LEVY, H. A. (1974). *International Tables for X-ray Crystallography*, Vol. IV, pp. 311–336. Birmingham: Kynoch Press. (Present distributor Kluwer Academic Publishers, Dordrecht.)
KUHS, W. F. (1983). *Acta Cryst.* A**39**, 148–158.
SCHOMAKER, V. & TRUEBLOOD, K. N. (1968). *Acta Cryst.* B**24**, 63–76.
SRINIVASAN, R. & JAGANNATHAN, N. R. (1982). *Acta Cryst.* B**38**, 2093–2095
STEINER, T., MASON, S. A. & SAENGER, W. (1990). *J. Am. Chem. Soc.* **112**, 6184–6190.
STEINER, T., MASON, S. A. & SAENGER, W. (1991). *J. Am. Chem. Soc.* **113**, 5676–5687.
STEINER, T. & SAENGER, W. (1992). *J. Am. Chem. Soc.* In the press.
WEBER, H.-P., CRAVEN, B. M. & MCMULLAN, R. K. (1983). *Acta Cryst.* B**39**, 360–366.
WEBER, H.-P., CRAVEN, B. M., SAWZIK, P. & MCMULLAN, R. K. (1991). *Acta Cryst.* B**47**, 116–127.

Acta Cryst. (1993). A**49**, 384–388

X-ray Diffraction when the Real Part of the Scattering Factor is Zero

BY TOMOE FUKAMACHI

Department of Electronic Engineering, Saitama Institute of Technology, Okabe, Saitama 369-02, *Japan*

AND TAKAAKI KAWAMURA

Department of Physics, Yamanashi University, Kofu, Yamanashi 400, *Japan*

(*Received* 13 *February* 1992; *accepted* 27 *May* 1992)

Abstract

A formulation of dynamical X-ray diffraction is given for use when studying X-ray diffraction intensities when the real part of the scattering factor is zero. Based on these formulae, the diffraction induced by the imaginary part of the scattering factor alone is studied for both the Bragg and Laue cases.

1. Introduction

Many studies using dynamical theories of X-ray diffraction (Zachariasen, 1945; James, 1963; Batterman & Cole, 1964; Miyake, 1969; Kato, 1974) have been carried out for absorbing crystals as well as for crystals without absorption. Some of the theories are not applicable to the case when the absorption is quite large or even the case when the real part of the scattering factor is zero. If we denote the normal scattering factor by f^0, which depends on the reciprocal-lattice vector **h**, and the real and the imaginary parts of the anomalous scattering factor by f' and f'', respectively, f'' is usually assumed to be small compared with $f^0 + f'$. By taking the absorption effect as a perturbation, most of the experimental

0108-7673/93/030384-05$06.00

observations have been explained even in the case of strong absorption.

With X-rays from a synchrotron-radiation source and a tuned X-ray energy ($\hbar\omega$), it is possible to make the real part of the scattering factor zero for some reflections from monoatomic crystals and some compound crystals. If the real part of the anomalous scattering factor $f'(\omega)$ is changed so as to make the value of $f^0(\mathbf{h})+f'(\omega)$ zero, the diffraction is induced by only the imaginary part of the anomalous scattering factor $f''(\omega)$.

In this paper, we give a formulation of dynamical X-ray diffraction that is applicable to general cases including the case when the real part of the scattering factor is zero and the imaginary part is nonzero. We calculate reflection intensities both in the Bragg case for semi-infinite crystals and in the Laue case.

2. Theory

The coherent scattering factor in a crystal is expressed by using the Fourier component of electron polarizability χ_h ($\times 4\pi$) in the atomic unit ($\hbar = m = e = 1$) as

$$\chi_h = \chi_{hr} + i\chi_{hi}. \tag{1}$$

The real and the imaginary parts are given to a good approximation by

$$\chi_{hr} = -(4\pi/v\omega^2)\sum_j (f_j^0 + f_j')\exp(i2\pi\mathbf{h}\cdot\mathbf{r}_j)T_j, \tag{2}$$

$$\chi_{hi} = -(4\pi/v\omega^2)\sum_j f_j''\exp(i2\pi\mathbf{h}\cdot\mathbf{r}_j)T_j. \tag{3}$$

Here, v is the volume of the unit cell, r_j is the position vector of the jth atom in a unit cell and T_j is the correction factor due to thermal vibration. By expressing the phases of χ_{hr} and χ_{hi} as α_{hr} and α_{hi}, respectively, the phase difference between the two is

$$\delta = \alpha_{hi} - \alpha_{hr}. \tag{4}$$

We write the product of χ_h and χ_{-h} as

$$\chi_h\chi_{-h} = |\chi_h|^2(1 - b^2 + i2p\cos\delta). \tag{5}$$

Here,

$$|\chi_h|^2 = |\chi_{hr}|^2 + |\chi_{hi}|^2, \tag{6}$$

$$b = 2^{1/2}|\chi_{hi}|/|\chi_h|, \tag{7}$$

$$p = |\chi_{hr}||\chi_{hi}|/|\chi_h|^2. \tag{8}$$

The parameter b has the minimum value zero when $\chi_{hi} = 0$ and the maximum value $2^{1/2}$ when $\chi_{hr} = 0$. The parameter p becomes zero when either χ_{hr} or χ_{hi} is zero. The dispersion surface in the two-beam approximation is shown in Fig. 1, which defines the X and Y axes. The resonance error W, which expresses the degree of difference from the exact Bragg condition, is given by

$$W = -X_0(\sin 2\theta)/[|(\cos\theta_1)(\cos\theta_2)|^{1/2}\kappa_{0r}|\chi_h|], \tag{9}$$

where θ is the diffraction angle and the parameters X_0, θ_1 and θ_2 are shown in Fig. 1. κ_{0r} is the real part of the wave vector inside the crystal. Note that W defined in this way is applicable to the cases in which either χ_{hr} or χ_{hi} is zero. To simplify the intensity formula, we define

$$g = \chi_{0i}/|\chi_h|, \tag{10}$$

$$g' = g(\sin\theta)(\cos\beta)/|(\cos\theta_1)(\cos\theta_2)|^{1/2}. \tag{11}$$

The quantity g is nonpositive.

In the following, we consider only the σ-polarization case. The discussion for π polarization is the same except that we multiply the polarizability χ_h by $|\cos 2\theta|$.

2.1. *The Bragg case*

The reflectively, *i.e.* the ratio of the diffraction intensity, P_h, and the incident intensity, P_0, is

$$P_h/P_0 = k[\Pi - (\Pi^2 - 1)^{1/2}], \tag{12}$$

where

$$k = (1 - 2p\sin\delta)/[(1-b^2)^2 + 4p^2\cos^2\delta]^{1/2}, \tag{13}$$

and

$$\Pi = \frac{[(A^2+B^2)^{1/2} + W^2 + g'^2]}{[(1-b^2)^2 + 4p^2\cos^2\delta]^{1/2}}. \tag{14}$$

In (14), A and B are given by

$$A = W^2 - 1 - g'^2 + b^2, \tag{15}$$

$$B = 2(g'W - p\cos\delta). \tag{16}$$

Owing to the factor $2p\sin\delta$ in (13), the reflection

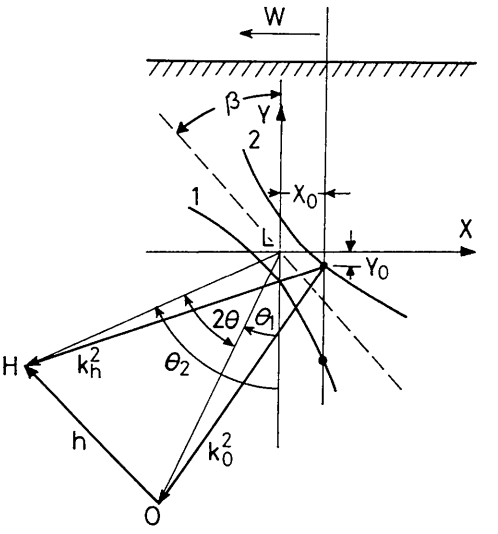

Fig. 1. Schematic diagram of the dispersion surface. The origin of the reciprocal vector is 0, the diffraction point is H and the Laue point is L. k_h^2 and k_0^2 are the wave vectors of the diffracted and the transmitted beams, respectively.

intensity P_h/P_0 from the front surface is different from that from the back surface for a polar crystal. When $\chi_{hr}=0$, P_h/P_0 becomes

$$P_h/P_0 = l-(l^2-1)^{1/2}, \tag{17}$$

where

$$l=[(W^2+1-g'^2)^2+4g'^2W^2]^{1/2}+W^2+g'^2. \tag{18}$$

If $\chi_{hr}=0$, the intensity in (17) does not have polarity dependence. The Friedel law holds if $\chi_{hi}=0$.

In Fig. 2, the reflectivities P_h/P_0 are shown as a function of W defined in (9) from -3 to 3 in the symmetric-reflection condition. When $\chi_{hr}=0$ and $g'=-1.0$, the rocking curve of reflectivity P_h/P_0 has the maximum value 1 when $W=0$ and is symmetric with respect to $W=0$ (curve 1). When $\chi_{hr}=0$, the minimum value of $|g'|$ is 1. By increasing $|g'|$, the peak height of the rocking curve becomes small. The rocking curve for $g'=-1.1$ is shown in curve 6.

Other rocking curves are also shown in Fig. 2 for the cases $|\chi_{hr}|=|\chi_{hi}|/2$ (curve 2), $|\chi_{hr}|=|\chi_{hi}|$ (curve 3), $|\chi_{hr}|=2|\chi_{hi}|$ (curve 4) and $|\chi_{hi}|=0$ (curve 5). The values of the parameters b, p and g for these cases are shown in Table 1. If $|\chi_{hr}|=0$, the rocking curve is maximum when $W=0$, as shown in curve 1. By increasing $|\chi_{hr}|/|\chi_{hi}|$, the peak position shifts to negative values of W, as shown in curves 2 to 4. When $|\chi_{0i}|=0$, P_h/P_0 is unity for W between -1 and 1. The change of the ratio $|\chi_{hr}|/|\chi_{hi}|$ corresponds to the change of X-ray energy just below the absorption edge: $|\chi_{hr}|$ changes greatly and $|\chi_{hi}|$ is almost constant.

As is well known (Hirsch & Ramachandran, 1950), the peak of the rocking curve decreases and the peak

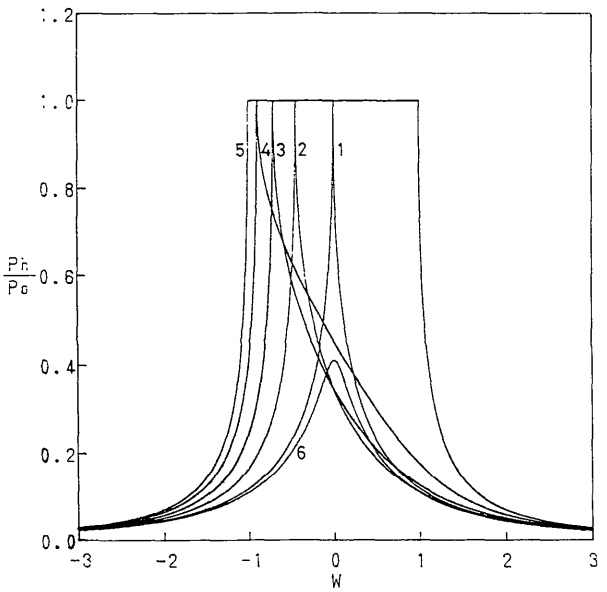

Fig. 2. The rocking curves from a semi-infinite crystal in the Bragg case. The values of b, p, g, χ_{hr} and χ_{hi} for curves 1 to 5 are given in Table 1. $\chi_{hr}=0$ and $g=-1.1$ for curve 6.

Table 1. *Parameter values and conditions on χ_{hr} and χ_{hi} for the curves in Fig. 2*

Curve	b	p	g	Condition
1	1.4142	0.0	−1.0	$\chi_{hr}=0$
2	1.2649	0.4	−0.8994	$\lvert\chi_{hr}\rvert=\lvert\chi_{hi}\rvert/2$
3	1.0	0.5	−0.7071	$\lvert\chi_{hr}\rvert=\lvert\chi_{hi}\rvert$
4	0.6325	0.4	−0.4472	$\lvert\chi_{hr}\rvert=2\lvert\chi_{hi}\rvert$
5	0.0	0.0	0.0	$\chi_{hi}=0$

position moves toward the center ($W=0$) with increasing $|g'|$ from 2 to 4 for each curve.

The integrated reflecting power in the angle-dispersive mode R_h is given by

$$R_h=(|\cos\theta_2|/\cos\theta_1)^{1/2}(|\chi_h|/\sin 2\theta)\int(P_h/P_0)\,\mathrm{d}W. \tag{19}$$

This formula is applicable to both the Bragg and the Laue cases. It is noted that the coefficient of (19) contains $|\chi_h|$ rather than $|\chi_{hr}|$ (Kato, 1968). In previous works such as that of Hirsch & Ramachandran (1950), R_h contains $|\chi_{hr}|$ in the coefficient and seems to be zero when $|\chi_{hr}|=0$, although it is not zero as is clearly seen in (19).

In the Bragg case when $|g'|\gg 1$, R_h has the same value as that given by Hirsch & Ramachandran and agrees with the value from a mosaic crystal. However, when $|\chi_{hr}|=0$, the reflecting power based on a dynamical theory that takes account of the absorption effect (Afanas'ev & Perstnev, 1969) is 20% larger than that from a mosaic crystal for $b=2^{1/2}$ and $|g'|=1.0$. The integrated reflecting power gives better agreement with that from a mosaic crystal when $|g'|$ is more than 2.0.

2.2. *The Laue case*

The reflectivity of the diffraction **h** is given by

$$P_h/P_0=\exp(-\mu H')(1-2p\sin\delta)[\sin^2(sH\ \mathrm{Re}\ L^{1/2}) + \sinh^2(sH\ \mathrm{Im}\ L^{1/2})]/|L^{1/2}|^2, \tag{20}$$

where H is the crystal thickness. The linear absorption coefficient μ is

$$\mu=-2\pi K_0\chi_{0i}, \tag{21}$$

where K_0 is the wave number. Instead of A in (15), we define A for the Laue case as

$$A=W^2+1-g'^2-b^2. \tag{22}$$

The quantity L in (22) is given by

$$|L^{1/2}|^2=(A^2+B^2)^{1/2}, \tag{23}$$

$$\mathrm{Re}\ L^{1/2}=[A+(A^2+B^2)^{1/2}]^{1/2}/2^{1/2}, \tag{24}$$

$$\mathrm{Im}\ L^{1/2}=\pm[-A+(A^2+B^2)^{1/2}]^{1/2}/2^{1/2}, \tag{25}$$

where B is the same as in (16). In (25), the $\pm$ sign means that we take the positive value when $g'W-p\cos\delta>0$ and the negative value when

$g'W - p\cos\delta < 0$. The parameters s and H' in (20) are given by

$$s = \pi\kappa_{0r}|\chi_h|/|(\cos\theta_1)(\cos\theta_2)|^{1/2}, \quad (26)$$

$$H' = H(\cos\theta)(\sin\beta)/(\cos\theta_1)(\cos\theta_2). \quad (27)$$

If we consider the symmetric reflection condition under $g' = 0$ and $\chi_{hr} = 0$, the reflectivity is simplified to

$$P_h/P_0 = \exp(-\mu H')\{\sin^2[sH(W^2-1)^{1/2}]\}/(W^2-1). \quad (28)$$

If we set $W = 0$, the reflectivity is expressed by

$$P_h/P_0 = \exp(-\mu H')[\exp(2sH) + \exp(-2sH) + 2]/4. \quad (29)$$

In (29), the first term gives the abnormal transmission and the second term gives the abnormal absorption. For $sH \gg 1$, (29) becomes

$$P_h/P_0 = \exp[-\mu H'(1+1/g)]/4 \quad (30)$$

and the abnormal transmission term becomes the maximum 0.25 when $|\chi_{hi}| = |\chi_{0i}|$, *i.e.* $g = -1$. The reflectivities calculated from (28) are shown in Fig. 3 for $g = -1.0$ by changing the thickness H. The value of sH is 0.5 for curve 1, 1.0 for curve 2 and 5.0 for curve 3. Since the rocking curves are symmetric with respect to $W = 0$, only curves for positive W are shown, in the range $0 \leq W \leq 12$. Each curve has its maximum when $W = 0$. With increasing sH, the peak value becomes large and the width of the peak becomes narrow owing to abnormal absorption. In the limit of large sH, the maximum value becomes 0.25, as can be seen from (30). In curves 1 and 2 in Fig. 3, peaks also appear for large W. These peak heights decrease with increasing sH. As clearly seen in Fig. 3, *Pendellösung* fringes are observed even when $\chi_{hr} = 0$, which means the value of $|\chi_{hi}|$ can be determined in this case by measuring the rocking curve. If $|g|$ is increased from 1.0 by increasing the temperature, each peak height decreases systematically but the position does not change.

In Fig. 4, the integrated reflecting powers in the Laue case are shown for six values of g as a function of sH when $|\chi_{hr}| = 0$. The curves are maximum around $sH = 0.5$ and decrease slowly when $|g| = 1.0$. For $|g| > 1.0$, the curves decrease steeply as sH increases from 1.0. It is noted that there are no *Pendellösung* fringes in these intensities. In practice, the values of g and $|\chi_{hi}|$ can be determined by measuring the integrated reflection intensities as a function of sH.

Next we discuss the transmitted beam intensity. If the transmitted X-ray intensity is denoted by P_d, P_d/P_0 is given by

$$\begin{aligned} P_d/P_0 = \exp(-\mu H') &\times\{[(|L|^2 - W^2 - g'^2)\cos(2sH\ \mathrm{Re}\ L^{1/2}) \\ &+ (|L|^2 + W^2 + g'^2)\cosh(2sH\ \mathrm{Im}\ L^{1/2})]/2 \\ &+ (g'\ \mathrm{Re}\ L^{1/2} - W\ \mathrm{Im}\ L^{1/2})\sin(2sH\ \mathrm{Re}\ L^{1/2}) \\ &+ (W\ \mathrm{Re}\ L^{1/2} + g'\ \mathrm{Im}\ L^{1/2}) \\ &\times\sinh(2sH\ \mathrm{Im}\ L^{1/2})\}/|L^{1/2}|^2. \end{aligned} \quad (31)$$

In the case of $\chi_{hr} = 0$ and the symmetric reflection, (31) is expressed by

$$P_d/P_0 = [\exp(-\mu H')/2]\{-\cos[2sH(W^2-1)^{1/2}] + 2W^2 - 1\}/(W^2-1). \quad (32)$$

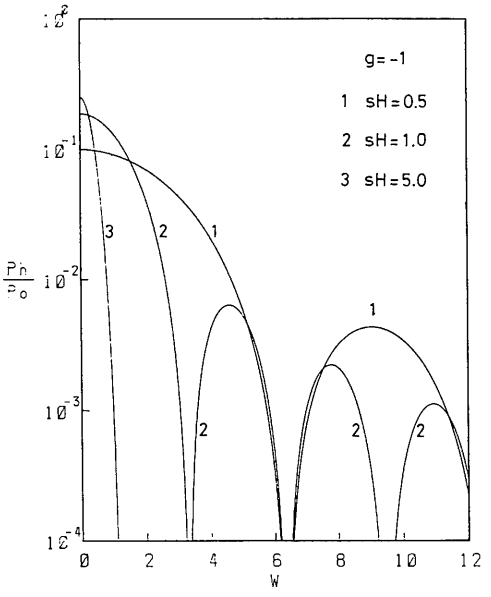

Fig. 3. The rocking curves of the diffracted beam in the Laue case for $\chi_{hi} = 0$ and different values of sH.

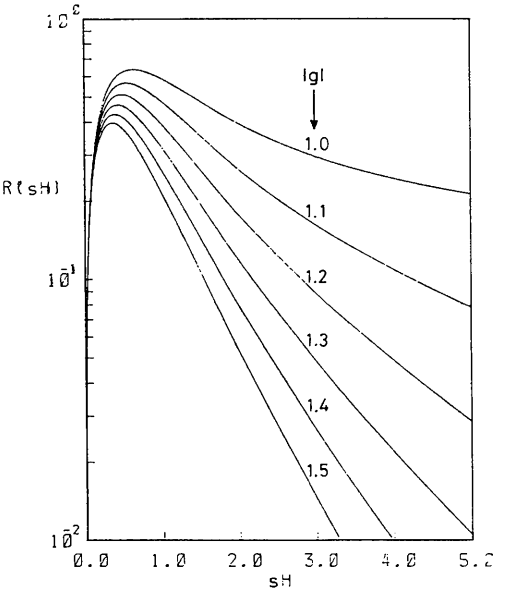

Fig. 4. The integrated reflecting powers $R(sH)$ of the diffracted beam in the Laue case for $\chi_{hi} = 0$ for different values of g. $R(sH)$ is given by the integration term of (19).

For $W=0$, (32) becomes

$$9P_d/P_0=[\exp(-\mu H')/2]\{[\exp(2sH)+\exp(-2sH)]/2-1\}. \quad (33)$$

The first term in (33) gives the abnormal transmission and the second term gives the abnormal absorption. For $sH \gg 1$, the abnormal transmission becomes 0.25, as for the diffracted beam. P_d/P_0 in (32) is symmetric with respect to $W=0$. The rocking curves calculated from (32) for $g=-1.0$ are shown in Fig. 5 for different values of sH. As sH increases, the width of the peak around $W=0$ becomes narrow and the peak becomes sharp. For large sH, *Pendellösung* fringes are clearly seen, although the intensities are quite small.

3. Summary

We have derived formulae for dynamical X-ray diffraction intensities that are applicable to the case of strong absorption when the real part of the scattering factor is zero ($\chi_{hr}=0$), as well as to the no-absorption case. Based on the formulae, we have discussed the diffraction by the imaginary part of the atomic scattering factor only, *i.e.* $\chi_{hr}=0$.

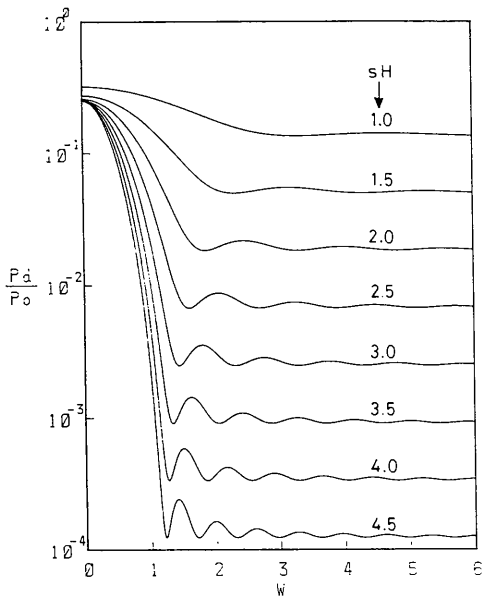

Fig. 5. The rocking curves of the transmitted beam in the Laue case for $\chi_{hi}=0$ and different values of sH.

We have obtained the following results. Firstly, for a polar crystal, the information on polarity is lost when $\chi_{hr}=0$ as it is when $\chi_{hi}=0$. The ratio of reflectivities from the front and the back surfaces is expected to be maximum when $|\chi_{hr}|=|\chi_{hi}|$ and the maximum value of p in (8) is 0.5. If either $|\chi_{hr}|$ or $|\chi_{hi}|$ becomes relatively large, the intensity ratio due to polarity becomes small.

Secondly, the integrated reflecting power in (19) has a finite value even when $|\chi_{hr}|$ is zero. In the Bragg case, the rocking cuve of the diffracted beam is quite sharp owing to the scattering factor $|\chi_{hi}|$ and is symmetric with respect to $W=0$. The integrated reflecting power is not always the same as that from a mosaic crystal, as reported in previous works, when $|\chi_{0i}|$ and $|\chi_{hi}|$ become large (Hirsch & Ramachandran, 1950).

Finally, in the Laue case, the rocking curves of both the transmitted and the diffracted beams are symmetric with respect to $W=0$ and show *Pendellösung* fringes. The abnormal transmission of 25% is observed in both of these beams when $g=-1.0$ and $sH>1$.

The authors thank M. Yoshizawa, K. Ehara and Professor T. Nakajima for their cooperation in the preliminary experiment at the Photon Factory, KEK, and R. Negishi for his help with calculations.

References

AFANAS'EV, A. M. & PERSTNEV, I. P. (1969). *Acta Cryst.* A**25**, 520-523.

BATTERMAN, B. W. & COLE, H. (1964). *Rev. Mod. Phys.* **36**, 681-717.

HIRSCH, P. B. & RAMACHANDRAN, G. N. (1950). *Acta Cryst.* **3**, 187-194.

JAMES, R. W. (1963). *Solid State Phys.* **15**, 53-220.

KATO, N. (1968). *J. Appl. Phys.* **19**, 2225-2230, 2231-2237.

KATO, N. (1974). In *X-ray Diffraction*, edited by L. V. AZAROFF, ch. 4 and Appendix 4A. New York: McGraw-Hill.

MIYAKE, S. (1969). *X-ray Diffraction.* Tokyo: Asakura. (In Japanese.)

ZACHARIASEN, W. H. (1945). *Theory of X-ray Diffraction in Crystals.* New York: Dover.